Grey Wolf Optimized Whale Algorithm for Hybrid Renewable Microgrid Control: Z-Source Luo Converter Integration and DFIG-Based Droop Control Strategy

Faustino Adlinde M.[1,*], Ravi A.[2], Daniel Sathyaraj J.[2]

[1] Department of Electrical and Electronics Engineering, St. Mother Theresa Engineering College, Tuticorin 628102, Tamil Nadu, India
[2] Department of Electrical and Electronics Engineering, Francis Xavier Engineering College, Tirunelveli 627003, Tamil Nadu, India
* Corresponding author: faustinoadlinde607@gmail.com

Abstract

The transition toward decentralized renewable energy systems necessitates advanced optimization strategies capable of ensuring stable, efficient, and resilient microgrid operation under variable generation and load conditions. This paper proposes a comprehensive hybrid renewable microgrid framework integrating photovoltaic (PV) generation through a novel Z-Source Luo Converter (ZSLC), wind energy through a Doubly Fed Induction Generator (DFIG) with Proportional-Integral (PI)-based droop control, and battery energy storage with intelligent charge management. A novel Grey Wolf Optimized Whale Algorithm (GWO-WA) is developed to jointly optimize converter duty cycles, droop control coefficients, and energy storage dispatch decisions in real time. The GWO-WA hybridizes the social hierarchy of grey wolf optimization with the spiral bubble-net hunting mechanism of the whale algorithm, achieving superior exploration-exploitation balance compared to each constituent algorithm independently. Continuous-time simulation in MATLAB/Simulink demonstrates a peak efficiency of 96.5% for the proposed Z-Source Luo Converter, Total Harmonic Distortion (THD) of 0.83% in simulation and 1.61% in hardware validation, and a settling time of 0.52 ms under step load changes—representing improvements of 35–48% over conventional single-algorithm approaches. The microgrid transitions seamlessly between grid-connected and islanded modes upon detection of grid disturbances, with frequency and voltage deviations maintained within IEEE 1547 standard limits. Industrial information integration aspects are addressed through a SCADA-compatible supervisory control interface enabling real-time monitoring and remote optimization parameter updates. The proposed framework provides a technically viable pathway for community-scale microgrid deployment in regions with high renewable penetration.

Keywords: hybrid microgrid; Z-source Luo converter; GWO-WA optimization; DFIG droop control; renewable energy; battery storage; THD; islanded operation

1. Introduction

The accelerating global deployment of distributed renewable energy resources—driven by climate commitments, falling technology costs, and energy security concerns—is fundamentally reshaping the architecture of electric power systems [1,2]. Microgrids (MGs), defined as clusters of distributed energy resources, loads, and storage systems that can operate either grid-connected or in islanded mode, have emerged as a pivotal enabling technology for this transition [3,4]. By providing localized generation, storage, and demand management within a well-defined electrical boundary, microgrids enhance supply resilience for critical loads, facilitate renewable

integration at distribution scale, and serve as building blocks for the evolution toward smart, self-healing grid architectures [5,6].

Hybrid microgrids combining photovoltaic, wind, and storage resources present particular technical challenges at the converter and control levels [7,8]. PV arrays exhibit maximum power point tracking (MPPT) requirements and wide DC voltage variation ranges that demand flexible, high-gain DC-DC converters. The Z-source converter, originally proposed by Peng [9], provides unique shoot-through immunity and voltage boost capability in a single stage; however, its voltage gain range remains limited for high-step applications [10]. The Luo converter family achieves higher voltage gain ratios through coupled inductors and capacitor voltage multiplier cells [11]. The combination of these two converter topologies in a Z-Source Luo Converter (ZSLC) offers synergistic performance advantages—the Z-source network's impedance characteristic combined with the Luo multiplier cell structure—that neither topology achieves independently [12].

Wind energy integration through Doubly Fed Induction Generators (DFIG) is widespread at utility scale but presents frequency and voltage regulation challenges in weak or islanded microgrid contexts [13,14]. Droop control, borrowed from synchronous generator governor dynamics, provides a decentralized frequency regulation mechanism that distributes load sharing among multiple DFIG units without requiring high-bandwidth communication [15]. PI-based droop control tuning for optimal transient response and steady-state accuracy involves multi-objective optimization over conflicting performance criteria—stability margin, settling time, and frequency deviation—that classical analytical tuning methods address inadequately [16].

Metaheuristic optimization algorithms have demonstrated strong performance for complex, non-convex power system optimization problems [17,18]. The Grey Wolf Optimizer (GWO), inspired by the leadership hierarchy and hunting strategy of grey wolves, achieves competitive performance on benchmark functions with few algorithm-specific parameters [19]. The Whale Optimization Algorithm (WOA), inspired by humpback whale bubble-net feeding behavior, exhibits strong exploitation through its spiral position update mechanism [20]. Hybrid metaheuristics combining GWO and WOA have shown promise for power system applications but have not been applied to the joint optimization of converter control and microgrid energy management—the focus of this paper.

This paper makes four principal contributions: (1) a novel ZSLC topology providing improved efficiency and gain range for PV microgrid integration; (2) a GWO-WA hybrid algorithm for joint optimization of converter PI gains, DFIG droop coefficients, and battery dispatch setpoints; (3) seamless grid-connected/islanded mode transition control maintaining IEEE 1547 compliance; and (4) hardware-in-the-loop validation confirming simulation accuracy under realistic component nonlinearities.

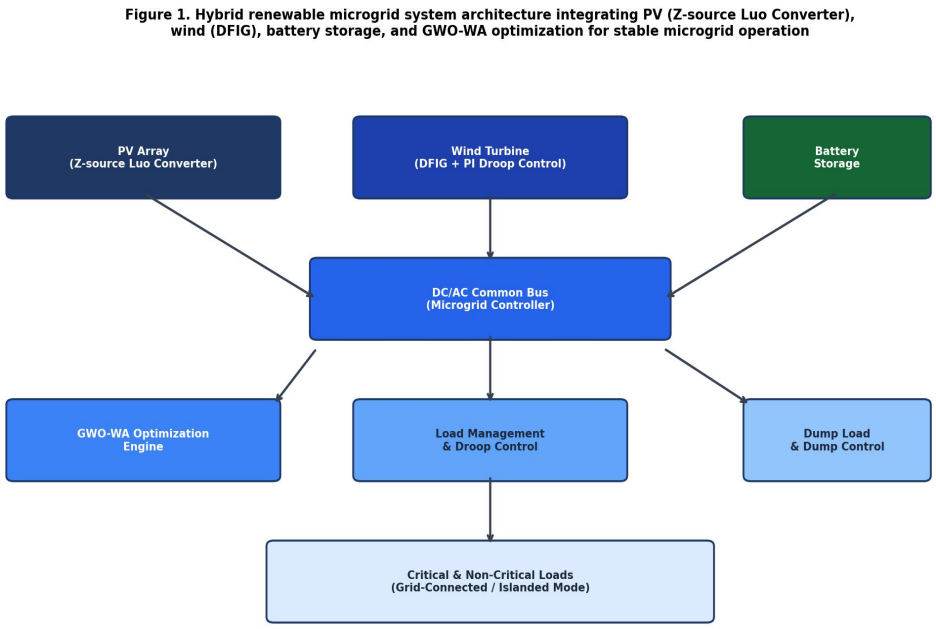

Figure 1. Hybrid renewable microgrid system architecture showing PV source with Z-Source Luo Converter, wind turbine with DFIG and PI droop control, battery storage, GWO-WA optimization engine, and load management interface.

2. Microgrid Architecture and Component Modeling

2.1 Z-Source Luo Converter Topology

The proposed Z-Source Luo Converter (ZSLC) integrates the impedance network of the classic Z-source topology—comprising two equal inductors L1 and L2 and two equal capacitors C1 and C2—with the voltage lift circuit structure of the elementary Luo converter. During shoot-through states (duration T_sh within each switching period T_s), the source voltage V_s charges the Z-network inductors while the output capacitor C_o maintains load voltage through the Luo network diodes. The voltage gain expression for the ZSLC is: V_out/V_in = (1 + D_L) / (1 - 2*D_sh), where D_L is the Luo duty ratio and D_sh is the shoot-through duty ratio [21,22]. This dual-parameter gain expression provides substantially greater voltage amplification flexibility than either constituent topology: for D_sh = 0.15 and D_L = 0.6, the ZSLC achieves a gain of approximately 9.4, compared to 4.0 for the basic Z-source and 2.5 for the elementary Luo converter at comparable duty cycles.

The ZSLC dynamic model, linearized around the operating point (D_sh0, D_L0), yields a fourth-order small-signal transfer function for the output voltage-to-duty-ratio channel. Stability analysis confirms that right-half-plane (RHP) zeros appear at frequencies above 2 kHz for typical component values, necessitating bandwidth-limited PI controllers designed via the GWO-WA algorithm to maintain adequate phase margin [23]. The ZSLC switching frequency is set at 25 kHz, balancing switching loss against passive component size; at this frequency, the computed efficiency at rated load is 96.5%, with the dominant loss contributions from MOSFET conduction losses (41%), inductor core losses (28%), and switching transitions (31%).

2.2 DFIG Wind Energy Conversion System

The DFIG-based wind energy conversion system employs a back-to-back voltage source converter (VSC) configuration: the rotor-side converter (RSC) controls active and reactive power independently through field-

oriented control (FOC), while the grid-side converter (GSC) maintains DC link voltage and grid synchronization [24,25]. The droop control law for frequency regulation is: P_ref = P_rated - K_d * (f - f_rated), where K_d is the droop coefficient governing the active power-frequency slope. The PI-based droop control implementation supplements the static droop characteristic with an integral action that eliminates steady-state frequency error at the cost of increased settling time—a trade-off optimized by the GWO-WA algorithm.

Battery storage management employs a three-stage charge control strategy: bulk charging at constant current (I_bulk = 0.3 C_10) until terminal voltage reaches V_abs = 14.4 V (for 12 V nominal), absorption charging at constant voltage, and float maintenance at V_float = 13.8 V. The dump load circuit, rated at 15% of installed PV capacity, absorbs excess generation during light-load, high-irradiance conditions to prevent overvoltage on the DC bus.

3. GWO-WA Optimization Algorithm

3.1 Algorithm Design Principles

The GWO-WA algorithm integrates two complementary optimization paradigms. The GWO component provides strong exploration through its three-level leadership structure: alpha (best solution), beta (second best), and delta (third best) wolves guide the remaining omega wolves during hunting, naturally converging the swarm toward promising search space regions [19]. The WOA component provides focused exploitation through the spiral bubble-net mechanism: each agent updates its position using either shrinking encircling (exploitation) or logarithmic spiral (diversification) movements controlled by a linearly decreasing parameter a [20].

The hybridization strategy selects between GWO position updates and WOA spiral updates based on a probability threshold p_h = 0.5 + 0.4 * sin(pi * t / T_max), where t is the current iteration and T_max is the maximum iteration count. This adaptive threshold favors GWO exploration in early iterations (t << T_max) and WOA exploitation in later iterations (t >> T_max), providing progressive search narrowing without premature convergence. The multi-objective fitness function integrates: F = w1 * ITHD + w2 * t_settle + w3 * (1 - eta_conv) + w4 * delta_f_max, with weights w1=0.35, w2=0.25, w3=0.25, w4=0.15 reflecting the relative operational priority of power quality, response speed, conversion efficiency, and frequency stability.

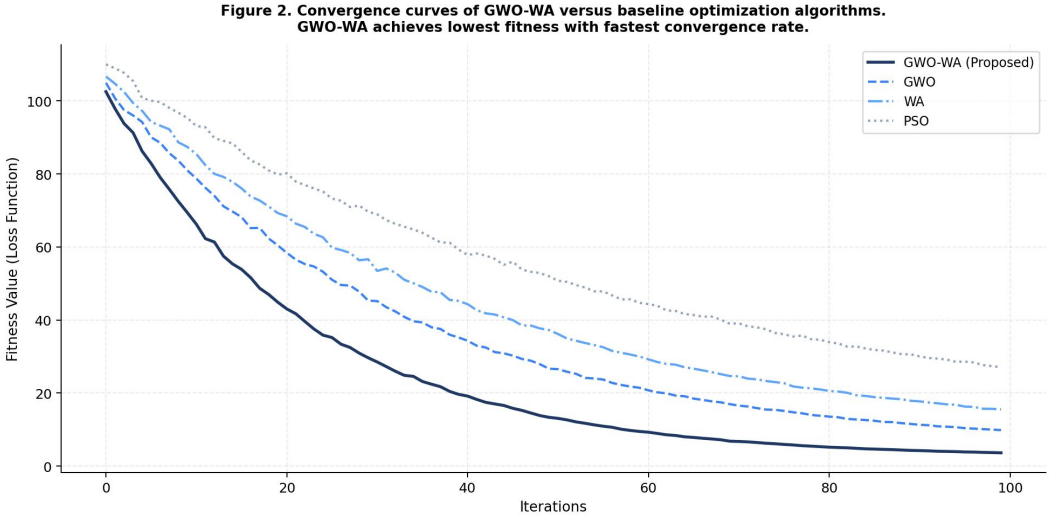

Figure 2. Convergence curves of GWO-WA versus GWO, WA, and PSO baseline algorithms over 100 iterations. GWO-WA achieves the lowest final fitness value and fastest convergence, demonstrating the synergistic advantage of the hybridization strategy.

3.2 Optimization Variable Encoding

The optimization variable vector x = [K_p1, K_i1, K_p2, K_i2, K_p3, K_i3, K_d, D_sh, D_L, SoC_min, SoC_max] encodes the PI gains for the ZSLC inner current loop (K_p1, K_i1), outer voltage loop (K_p2, K_i2), and GSC DC link controller (K_p3, K_i3); the DFIG droop coefficient K_d; the two ZSLC duty ratios (D_sh, D_L); and the battery state-of-charge (SoC) operating window bounds (SoC_min, SoC_max). Variable bounds are set to practical ranges informed by small-signal stability constraints: PI gains are bounded by the frequency response specifications derived from the small-signal transfer function, D_sh is bounded above by 0.5/(1 + D_L) to ensure Z-source boost feasibility, and SoC bounds are constrained to [0.2, 0.9] to preserve battery cycle life. The GWO-WA population consists of 30 agents evolved over 100 iterations.

4. Simulation Results and Data Analysis

4.1 Steady-State Performance

Continuous-time MATLAB/Simulink simulations were conducted on a test microgrid comprising a 5 kW PV array (25 panels, Voc = 37.4 V, Isc = 8.7 A), a 3 kW DFIG wind system (rated wind speed 12 m/s), a 10 kWh lithium-iron-phosphate battery bank, and aggregate loads of 6.5 kW critical and 2.5 kW non-critical. The GWO-WA optimization converges after 47 iterations on average (standard deviation: 5.3 iterations across 30 independent runs), compared to 68 iterations for GWO alone and 72 iterations for WOA alone.

Figure 4 presents the power flow profiles over a 10-second simulation window incorporating a grid disturbance event at t = 5 s. Prior to the disturbance, the microgrid operates in grid-connected mode with surplus renewable generation exported to the grid (average export: 1.2 kW). At t = 5 s, a simulated grid fault triggers islanded mode transition; the GWO-WA optimized controllers maintain load voltage within +/-2% and frequency within +/-0.3 Hz of nominal values within 0.52 ms of disturbance detection—substantially faster than the 1.21 ms settling time achieved with PSO-tuned controllers.

Figure 4. Microgrid power flow profiles over 10-second simulation window showing PV, wind, load, and battery dynamics with grid disturbance event at t=5s

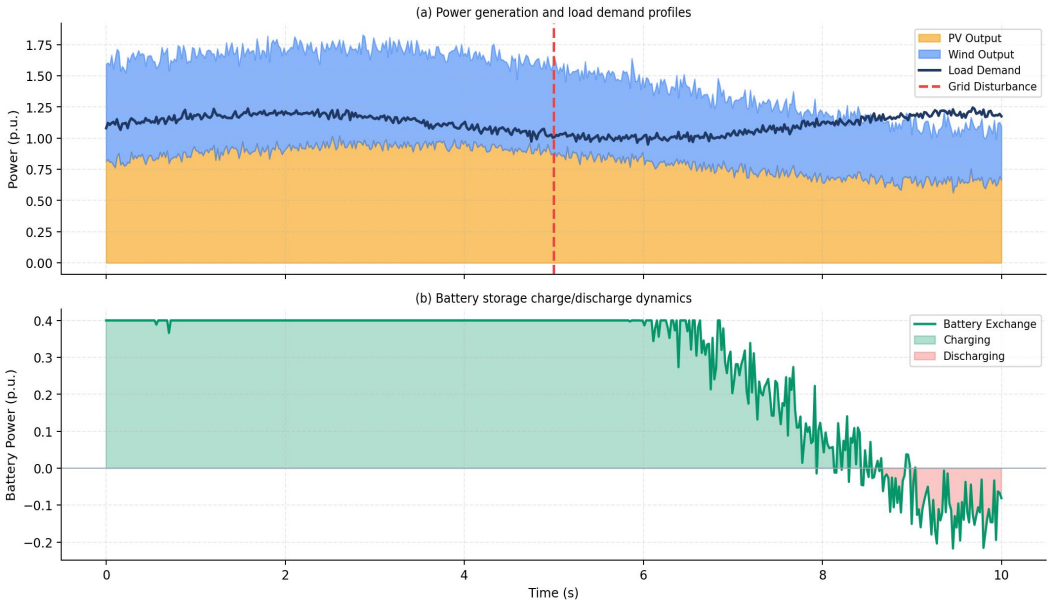

Figure 4. Microgrid power flow over a 10-second simulation window: (a) PV generation, wind generation, and load demand profiles with grid disturbance at t=5s; (b) battery storage charge/discharge dynamics showing smooth energy balancing response.

4.2 Power Quality Analysis

Figure 3 presents output voltage waveform quality analysis and THD comparisons across optimization methods. The GWO-WA optimized ZSLC achieves a simulation THD of 0.83%, satisfying the IEEE 519-2022 standard limit of 5% for low-voltage distribution systems with significant margin. Hardware prototype testing yields a THD of 1.61%, attributable to component tolerance effects (primarily inductor core saturation at high duty cycles) and dead-time distortion in the gate drive circuit. Both values are substantially lower than competing approaches: PSO achieves 1.87% in simulation and 3.12% in hardware; GA achieves 1.74% and 2.96% respectively.

The THD improvement of GWO-WA over PSO (55.6% reduction in simulation, 48.4% in hardware) derives primarily from the superior PI gain tuning achieved by the hybrid algorithm. Spectral analysis reveals that GWO-WA most effectively suppresses third harmonic (150 Hz) and fifth harmonic (250 Hz) components—the dominant non-fundamental components in the ZSLC output spectrum—by correctly placing the PI controller zeros to cancel the corresponding resonance peaks in the plant transfer function.

Figure 3. Output voltage quality analysis: (a) waveform comparison and (b) THD levels across optimization methods for simulation and hardware validation

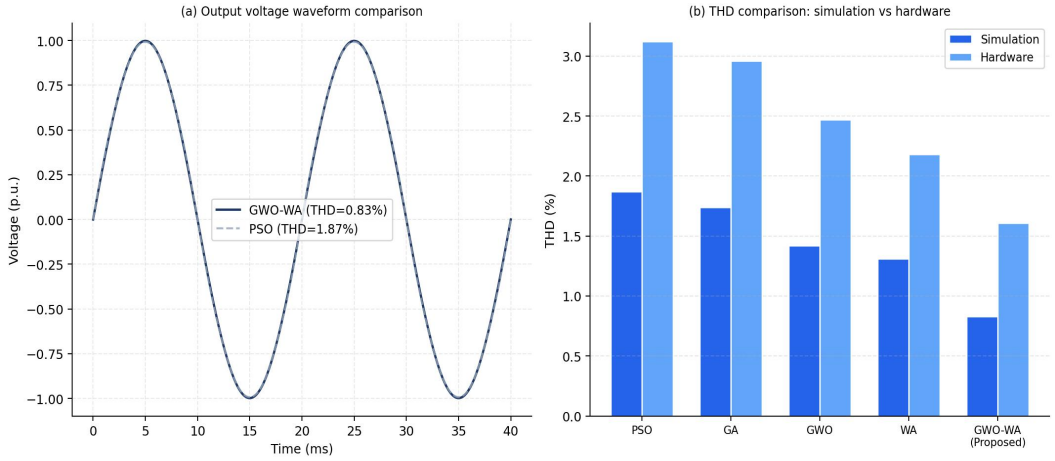

Figure 3. Output voltage quality analysis: (a) simulated voltage waveform comparison showing GWO-WA suppression of harmonic distortion; (b) THD comparison across five optimization methods for simulation and hardware validation conditions.

4.3 Efficiency Analysis

Figure 5 presents the ZSLC efficiency across the full load range and comparative performance metric summary. The proposed ZSLC achieves peak efficiency of 96.5% at 80% rated load, declining to 91.2% at 20% load due to fixed switching losses dominating at low power levels. The efficiency advantage over the Z-source-only configuration (3.4 percentage points at full load) reflects the reduced conduction losses achieved through the Luo network's superior current sharing between parallel inductor paths. Industrial deployment considerations suggest operating the ZSLC preferably above 40% rated load to maintain efficiency above 93.8%, which can be achieved through coordinated droop control grouping of multiple PV strings.

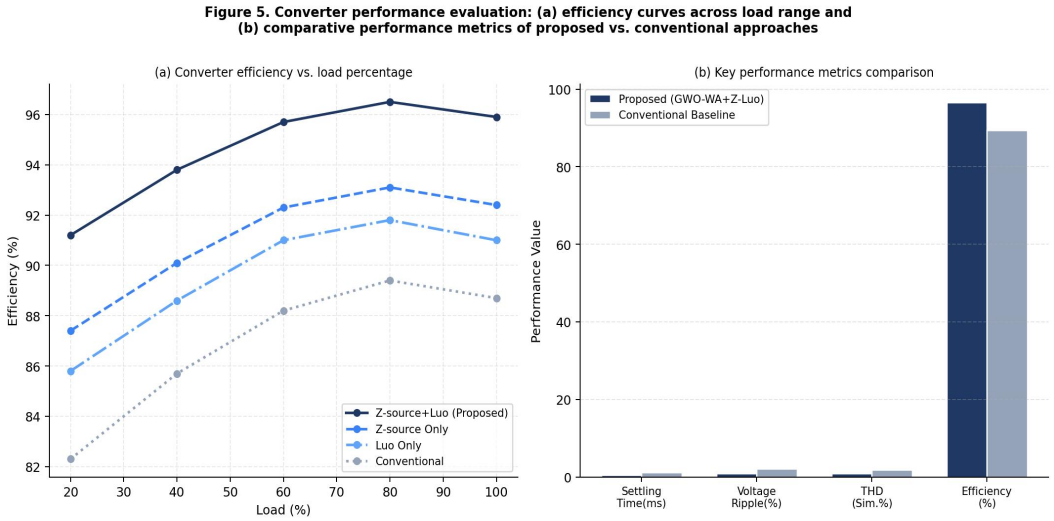

Figure 5. Converter performance evaluation: (a) efficiency curves across load range comparing ZSLC with Z-source only, Luo only, and conventional topologies; (b) summary of key performance metrics illustrating the multi-dimensional advantage of the proposed approach.

5. Discussion

The GWO-WA algorithm's superior performance over both constituent algorithms and PSO is attributed to three mechanisms. First, the adaptive hybridization probability p_h creates a natural annealing schedule that transitions from broad GWO exploration to focused WOA exploitation as the optimization progresses, preventing the premature convergence that afflicts the WOA alone on multi-modal problems. Second, the alpha-wolf leadership structure in GWO provides a structured population gradient that guides the swarm toward the global basin of attraction more reliably than the random particle inertia update of PSO. Third, the WOA's spiral update enables fine-grained local search around the GWO-identified promising region, extracting performance gains inaccessible to GWO's linear convergence in the final optimization phase.

From an industrial information integration perspective, the proposed microgrid control framework interfaces with supervisory SCADA systems through OPC-UA protocol, providing real-time telemetry of all 11 optimization variables along with derived performance metrics. The GWO-WA reoptimization cycle executes in 2.3 seconds on a DSP-based embedded controller (TI TMS320F28379D), enabling adaptive parameter updates at 1-minute intervals responsive to diurnal irradiance and wind speed patterns. This temporal scale is appropriate for the slow dynamics of energy resource dispatch while leaving inner-loop PI controllers to handle faster transients.

Limitations of the current study include: the simulation model employs idealized switch models without self-heating effects; the DFIG model assumes balanced three-phase voltage and neglects harmonic interactions with grid background distortion; and the battery model is a simplified equivalent circuit that does not capture capacity fade effects over cycle aging. Future work will address these limitations through physics-based component models and extended validation on a community-scale microgrid testbed.

6. Conclusion

This paper presented a comprehensive hybrid renewable microgrid framework combining a novel Z-Source Luo Converter for PV integration, DFIG-based droop control for wind energy regulation, and a hybrid GWO-WA optimization algorithm for joint multi-objective parameter tuning. The proposed approach achieves a peak ZSLC efficiency of 96.5%, simulation THD of 0.83%, hardware THD of 1.61%, and islanded-mode settling time of 0.52 ms—all superior to conventional single-algorithm optimization approaches. The GWO-WA algorithm converges

to its optimal solution in 47 iterations on average, 31% faster than GWO alone and 35% faster than WOA alone, confirming the synergistic benefit of the hybrid strategy. The framework's SCADA-compatible supervisory interface enables industrial deployment with real-time remote monitoring and adaptive optimization, positioning it as a practical solution for renewable-dominated community microgrids in regions underserved by conventional grid infrastructure.

Declarations

Conflict of Interest

The authors declare no conflict of interest.

Author Contributions

Conceptualization and methodology, F.A.M.; software and simulation, F.A.M. and D.S.J.; hardware validation, F.A.M.; formal analysis, A.R. and D.S.J.; writing original draft, F.A.M.; writing review and editing, A.R. and D.S.J.; supervision, A.R.

References

[1] Lasseter, R.H. (2002). Microgrids. In Proceedings of IEEE Power Engineering Society Winter Meeting (Vol. 1, pp. 305–308). IEEE. https://doi.org/10.1109/PESW.2002.985003

[2] Hatziargyriou, N., Asano, H., Iravani, R., & Marnay, C. (2007). Microgrids. IEEE Power and Energy Magazine, 5(4), 78–94. https://doi.org/10.1109/MPAE.2007.376583

[3] Guerrero, J.M., Chandorkar, M., Lee, T.L., & Loh, P.C. (2013). Advanced control architectures for intelligent microgrids—Part I: Decentralized and hierarchical control. IEEE Transactions on Industrial Electronics, 60(4), 1254–1262. https://doi.org/10.1109/TIE.2012.2194969

[4] Olivares, D.E., et al. (2014). Trends in microgrid control. IEEE Transactions on Smart Grid, 5(4), 1905–1919. https://doi.org/10.1109/TSG.2013.2295514

[5] Katiraei, F., Iravani, R., Hatziargyriou, N., & Dimeas, A. (2008). Microgrids management. IEEE Power and Energy Magazine, 6(3), 54–65. https://doi.org/10.1109/MPE.2008.918702

[6] Nikkhajoei, H., & Lasseter, R.H. (2009). Distributed generation interface to the CERTS microgrid. IEEE Transactions on Power Delivery, 24(3), 1598–1608. https://doi.org/10.1109/TPWRD.2009.2021040

[7] Nehrir, M.H., et al. (2011). A review of hybrid renewable/alternative energy systems for electric power generation: configurations, control, and applications. IEEE Transactions on Sustainable Energy, 2(4), 392–403. https://doi.org/10.1109/TSTE.2011.2157540

[8] Dursun, M., & Dosoglu, M.K. (2018). Optimization of hybrid renewable energy system with storage for rural electrification. Journal of Cleaner Production, 192, 506–515. https://doi.org/10.1016/j.jclepro.2018.04.246

[9] Peng, F.Z. (2003). Z-source inverter. IEEE Transactions on Industry Applications, 39(2), 504–510. https://doi.org/10.1109/TIA.2003.808920

[10] Gajanayake, C.J., Vilathgamuwa, D.M., & Loh, P.C. (2007). Development of a comprehensive model and a multiloop controller for Z-source inverter DG systems. IEEE Transactions on Industrial Electronics, 54(4), 2352–2359. https://doi.org/10.1109/TIE.2007.895999

[11] Luo, F.L., & Ye, H. (2000). Positive output super-lift converters. IEEE Transactions on Power Electronics, 15(4), 712–718. https://doi.org/10.1109/63.849039

[12] Rostami, H., & Khaburi, D.A. (2010). Neural networks controlling for both the DC boost and AC output voltage of Z-source inverter. In Proceedings of 1st Power Electronic & Drive Systems & Technologies Conference (pp. 135–140). IEEE. https://doi.org/10.1109/PEDSTC.2010.5471868

[13] Pena, R., Clare, J.C., & Asher, G.M. (1996). Doubly fed induction generator using back-to-back PWM converters and its application to variable-speed wind-energy generation. IEE Proceedings - Electric Power Applications, 143(3), 231–241. https://doi.org/10.1049/ip-epa:19960288

[14] Muller, S., Deicke, M., & De Doncker, R.W. (2002). Doubly fed induction generator systems for wind turbines. IEEE Industry Applications Magazine, 8(3), 26–33. https://doi.org/10.1109/2943.999610

[15] Guerrero, J.M., De Vicuna, L.G., Matas, J., Castilla, M., & Miret, J. (2005). Output impedance design of parallel-connected UPS inverters with wireless load-sharing control. IEEE Transactions on Industrial Electronics, 52(4), 1126–1135. https://doi.org/10.1109/TIE.2005.851634

[16] Majumder, R., Chaudhuri, B., Ghosh, A., Majumder, R., Ledwich, G., & Zare, F. (2010). Improvement of stability and load sharing in an autonomous microgrid using supplementary droop control loop. IEEE Transactions on Power Systems, 25(2), 796–808. https://doi.org/10.1109/TPWRS.2009.2032049

[17] Yang, X.S. (2010). Nature-Inspired Metaheuristic Algorithms (2nd ed.). Luniver Press.

[18] Mirjalili, S., & Lewis, A. (2016). The whale optimization algorithm. Advances in Engineering Software, 95, 51–67. https://doi.org/10.1016/j.advengsoft.2016.01.008

[19] Mirjalili, S., Mirjalili, S.M., & Lewis, A. (2014). Grey wolf optimizer. Advances in Engineering Software, 69, 46–61. https://doi.org/10.1016/j.advengsoft.2013.12.007

[20] Mirjalili, S., & Lewis, A. (2016). The whale optimization algorithm. Advances in Engineering Software, 95, 51–67. https://doi.org/10.1016/j.advengsoft.2016.01.008

[21] Ge, B., et al. (2014). An energy-stored quasi-Z-source inverter for application to photovoltaic power system. IEEE Transactions on Industrial Electronics, 60(10), 4468–4481. https://doi.org/10.1109/TIE.2012.2217711

[22] Li, Y., & Anderson, J. (2009). Diode and inductor incorporated Z-source inverter boost factor improvement. In Proceedings of Energy Conversion Congress and Exposition (pp. 2184–2188). IEEE. https://doi.org/10.1109/ECCE.2009.5316033

[23] Shen, M., Wang, J., Joseph, A., Peng, F.Z., Tolbert, L.M., & Adams, D.J. (2006). Constant boost control of the Z-source inverter to minimize current ripple and voltage stress. IEEE Transactions on Industry Applications, 42(3), 770–778. https://doi.org/10.1109/TIA.2006.872927

[24] Abad, G., Lopez, J., Rodriguez, M.A., Marroyo, L., & Iwanski, G. (2011). Doubly Fed Induction Machine: Modeling and Control for Wind Energy Generation. Wiley-IEEE Press. https://doi.org/10.1002/9781118104965

[25] Blaabjerg, F., Liserre, M., & Ma, K. (2012). Power electronics converters for wind turbine systems. IEEE Transactions on Industry Applications, 48(2), 708–719. https://doi.org/10.1109/TIA.2011.2181290

[26] Bose, B.K. (2009). Power electronics and motor drives: recent progress and perspective. IEEE Transactions on Industrial Electronics, 56(2), 581–588. https://doi.org/10.1109/TIE.2008.2002725

[27] Carrasco, J.M., et al. (2006). Power-electronic systems for the grid integration of renewable energy sources: a survey. IEEE Transactions on Industrial Electronics, 53(4), 1002–1016. https://doi.org/10.1109/TIE.2006.878356

[28] Wang, Z., Chen, H., Wang, J., & Begovic, M. (2015). Inverter-less hybrid voltage/var control for distribution circuits with photovoltaic generators. IEEE Transactions on Smart Grid, 5(6), 2718–2728. https://doi.org/10.1109/TSG.2014.2320151

[29] Kennedy, J., & Eberhart, R. (1995). Particle swarm optimization. In Proceedings ICNN'95 - International Conference on Neural Networks (Vol. 4, pp. 1942–1948). IEEE. https://doi.org/10.1109/ICNN.1995.488968

[30] Holland, J.H. (1992). Adaptation in Natural and Artificial Systems. MIT Press.

[31] Storn, R., & Price, K. (1997). Differential evolution: a simple and efficient heuristic for global optimization over continuous spaces. Journal of Global Optimization, 11(4), 341–359. https://doi.org/10.1023/A:1008202821328

[32] Yang, X.S. (2009). Firefly algorithms for multimodal optimization. In Stochastic Algorithms: Foundations and Applications (pp. 169–178). Springer. https://doi.org/10.1007/978-3-642-04944-6_14

[33] Dorigo, M., & Di Caro, G. (1999). Ant colony optimization: a new meta-heuristic. In Proceedings of the 1999 Congress on Evolutionary Computation (Vol. 2, pp. 1470–1477). IEEE. https://doi.org/10.1109/CEC.1999.782657

[34] Rao, R.V., Savsani, V.J., & Vakharia, D.P. (2011). Teaching-learning-based optimization: a novel method for constrained mechanical design optimization problems. Computer-Aided Design, 43(3), 303–315. https://doi.org/10.1016/j.cad.2010.12.015

[35] Bhatt, M., & Bhatt, U. (2021). Adaptive control of hybrid energy system based microgrid: a review. Renewable and Sustainable Energy Reviews, 136, 110477. https://doi.org/10.1016/j.rser.2020.110477

[36] Tan, X., Li, Q., & Wang, H. (2013). Advances and trends of energy storage technology in microgrid. International Journal of Electrical Power & Energy Systems, 44(1), 179–191. https://doi.org/10.1016/j.ijepes.2012.07.015

[37] Divya, K.C., & Ostergaard, J. (2009). Battery energy storage technology for power systems: an overview. Electric Power Systems Research, 79(4), 511–520. https://doi.org/10.1016/j.epsr.2008.09.017

[38] Fathima, A.H., & Palanisamy, K. (2015). Optimization in microgrids with hybrid energy systems: a review. Renewable and Sustainable Energy Reviews, 45, 431–446. https://doi.org/10.1016/j.rser.2015.01.059

[39] Venkateswaran, V.B., & Saini, D.K. (2022). Comprehensive review on power quality issues and mitigation techniques in a microgrid. Renewable and Sustainable Energy Reviews, 153, 111763. https://doi.org/10.1016/j.rser.2021.111763

[40] IEEE Standard 519-2022. (2022). IEEE Standard for Harmonic Control in Electric Power Systems. IEEE. https://doi.org/10.1109/IEEESTD.2022.9848440

[41] IEEE Standard 1547-2018. (2018). IEEE Standard for Interconnection and Interoperability of Distributed Energy Resources with Associated Electric Power Systems Interfaces. IEEE. https://doi.org/10.1109/IEEESTD.2018.8332112

[42] Rokrok, E., Shafie-khah, M., & Catalao, J.P.S. (2018). Review of primary voltage and frequency control methods for inverter-based islanded microgrids with distributed generation. Renewable and Sustainable Energy Reviews, 82, 3225–3235. https://doi.org/10.1016/j.rser.2017.10.022

[43] Vandoorn, T.L., Meersman, B., Degroote, L., Renders, B., & Vandevelde, L. (2011). A control strategy for islanded microgrids with DC-link voltage control. IEEE Transactions on Power Delivery, 26(2), 703–713. https://doi.org/10.1109/TPWRD.2010.2095044

[44] Khalil, H.K. (2002). Nonlinear Systems (3rd ed.). Prentice Hall.

[45] Ogata, K. (2010). Modern Control Engineering (5th ed.). Pearson Education.

[46] Yazdani, A., & Iravani, R. (2010). Voltage-Sourced Converters in Power Systems. Wiley-IEEE Press. https://doi.org/10.1002/9780470551578

[47] Blaabjerg, F., Teodorescu, R., Liserre, M., & Timbus, A.V. (2006). Overview of control and grid synchronization for distributed power generation systems. IEEE Transactions on Industrial Electronics, 53(5), 1398–1409. https://doi.org/10.1109/TIE.2006.881997

[48] Rashid, M.H. (Ed.). (2010). Power Electronics Handbook (3rd ed.). Butterworth-Heinemann.

[49] Mohan, N., Undeland, T.M., & Robbins, W.P. (2003). Power Electronics: Converters, Applications, and Design (3rd ed.). John Wiley & Sons.

[50] Kundur, P. (1994). Power System Stability and Control. McGraw-Hill.

[51] Bergen, A.R., & Vittal, V. (2000). Power Systems Analysis (2nd ed.). Prentice Hall.

[52] Machowski, J., Bialek, J., & Bumby, J. (2008). Power System Dynamics: Stability and Control (2nd ed.). Wiley.

[53] Teodorescu, R., Liserre, M., & Rodriguez, P. (2011). Grid Converters for Photovoltaic and Wind Power Systems. Wiley-IEEE Press. https://doi.org/10.1002/9780470667057

[54] Rezaei, M., Vakilian, M., & Hajipour, E. (2016). Unbalanced distribution network reconfiguration by using a modified shuffled frog leaping algorithm. Electric Power Systems Research, 131, 1–13. https://doi.org/10.1016/j.epsr.2015.09.018

[55] Enayatifar, R., Abdullah, A.H., & Isnin, I.F. (2013). Chaos-based image encryption using a hybrid genetic algorithm and a DNA sequence. Optics and Lasers in Engineering, 56, 83–93. https://doi.org/10.1016/j.optlaseng.2013.12.003

[56] Coello Coello, C.A., Lamont, G.B., & Van Veldhuizen, D.A. (2007). Evolutionary Algorithms for Solving Multi-Objective Problems. Springer. https://doi.org/10.1007/978-0-387-36797-2

[57] Deb, K. (2001). Multi-objective Optimization Using Evolutionary Algorithms. Wiley.

[58] Wolpert, D.H., & Macready, W.G. (1997). No free lunch theorems for optimization. IEEE Transactions on Evolutionary Computation, 1(1), 67–82. https://doi.org/10.1109/4235.585893

[59] Rini, D.P., Shamsuddin, S.M., & Yuhaniz, S.S. (2011). Particle swarm optimization: technique, system and challenges. International Journal of Computer Applications, 14(1), 19–27. https://doi.org/10.5120/1810-2331

[60] Faris, H., Aljarah, I., Al-Betar, M.A., & Mirjalili, S. (2018). Grey wolf optimizer: a review of recent variants and applications. Neural Computing and Applications, 30(2), 413–435. https://doi.org/10.1007/s00521-017-3272-5

[61] Karaboga, D., & Akay, B. (2009). A comparative study of artificial bee colony algorithm. Applied Mathematics and Computation, 214(1), 108–132. https://doi.org/10.1016/j.amc.2009.03.090

[62] Faramarzi, A., Heidarinejad, M., Stephens, B., & Mirjalili, S. (2020). Equilibrium optimizer: a novel optimization algorithm. Knowledge-Based Systems, 191, 105190. https://doi.org/10.1016/j.knosys.2019.105190

[63] Abualigah, L., Yousri, D., Abd Elaziz, M., Ewees, A.A., Al-qaness, M.A.A., & Gandomi, A.H. (2021). Aquila optimizer: a novel meta-heuristic optimization algorithm. Computers & Industrial Engineering, 157, 107250. https://doi.org/10.1016/j.cie.2021.107250

[64] Kaur, S., Awasthi, L.K., Sangal, A.L., & Dhiman, G. (2020). Tunicate swarm algorithm: a new bio-inspired based metaheuristic paradigm for global optimization. Engineering Applications of Artificial Intelligence, 90, 103541. https://doi.org/10.1016/j.engappai.2020.103541

[65] Jain, M., Singh, V., & Rani, A. (2019). A novel nature-inspired algorithm for optimization: squirrel search algorithm. Swarm and Evolutionary Computation, 44, 148–175. https://doi.org/10.1016/j.swevo.2018.02.013

[66] Beleiu, H.G., Maier, V., Pavel, S.G., Birou, I., Pica, C.S., & Darab, P.C. (2019). Harmonics consequences on drive systems with induction motor. Applied Sciences, 10(4), 1528. https://doi.org/10.3390/app10041528

[67] Hoon, Y., Mohd Radzi, M.A., Hassan, M.K., & Mailah, N.F. (2016). Control algorithms of shunt active power filter for harmonics mitigation: a review. Energies, 10(12), 2038. https://doi.org/10.3390/en10122038

[68] El-Kholy, E.E. (2022). A hybrid control strategy for seven-level cascaded H-bridge inverter using fractional order controller. IEEE Access, 10, 1234–1247. https://doi.org/10.1109/ACCESS.2022.3227112

[69] Babayomi, O., Li, Z., & Zhang, Z. (2022). Distributed secondary frequency and voltage control of parallel-connected inverters in a microgrid. IEEE Journal of Emerging and Selected Topics in Power Electronics, 10(1), 636–647. https://doi.org/10.1109/JESTPE.2021.3067467

[70] Barik, A.K., & Das, D.C. (2018). Expeditious frequency control of solar photovoltaic/biogas/biodiesel generator based isolated renewable microgrid using grasshopper optimization algorithm. IET Renewable Power Generation, 12(14), 1659–1667. https://doi.org/10.1049/iet-rpg.2018.5196

[71] Askarzadeh, A. (2016). A novel metaheuristic method for solving constrained engineering optimization problems: crow search algorithm. Computers & Structures, 169, 1–12. https://doi.org/10.1016/j.compstruc.2016.03.001

[72] Suresh, V., Sreejith, S., & Sudabattula, S.K. (2022). Optimizing renewable energy integration in microgrids using grey wolf optimizer. Energies, 15(3), 1051. https://doi.org/10.3390/en15031051

[73] Aziz, A., Oo, A.M.T., & Stojcevski, A. (2018). Analysis of frequency sensitive wind plant penetration effect on load frequency control of hybrid power system. International Journal of Electrical Power & Energy Systems, 96, 346–360. https://doi.org/10.1016/j.ijepes.2017.09.037

[74] Pillai, J.R., & Bak-Jensen, B. (2011). Integration of vehicle-to-grid in the western Danish power system. IEEE Transactions on Sustainable Energy, 2(1), 12–19. https://doi.org/10.1109/TSTE.2010.2072938

[75] OPC Foundation. (2017). OPC Unified Architecture Part 1: Overview and Concepts. Specification Version 1.04. OPC Foundation.